SCIENCE CHINA
Life Sciences

•RESEARCH PAPER•

March 2023 Vol.66 No.3: 602–611
https://doi.org/10.1007/s11427-022-2193-3

Plant Intron-Splicing Efficiency Database (PISE): exploring splicing of ~1,650,000 introns in *Arabidopsis*, maize, rice, and soybean from ~57,000 public RNA-seq libraries

Hong Zhang[1,2,3], Jinbu Jia[1,2,3] & Jixian Zhai[1,2,3*]

[1]*Department of Biology, School of Life Sciences, Southern University of Science and Technology, Shenzhen 518055, China;*
[2]*Institute of Plant and Food Science, Southern University of Science and Technology, Shenzhen 518055, China;*
[3]*Key Laboratory of Molecular Design for Plant Cell Factory of Guangdong Higher Education Institutes, Institute of Plant and Food Science, Department of Biology, Southern University of Science and Technology, Shenzhen 518055, China*

Received August 5, 2022; accepted August 30, 2022; published online November 18, 2022

Intron retention is the most common alternative splicing event in plants and plays a crucial role in the responses of plants to environmental signals. Despite a large number of RNA-seq libraries from different treatments and genetic mutants stored in public domains, a resource for querying the intron-splicing ratio of individual intron is still required. Here, we established the first-ever large-scale splicing efficiency database in any organism. Our database includes over 57,000 plant public RNA-seq libraries, comprising 25,283 from *Arabidopsis*, 17,789 from maize, 10,710 from rice, and 3,974 from soybean, and covers a total of 1.6 million introns in these four species. In addition, we manually curated and annotated all the mutant- and treatment-related libraries as well as their matched controls included in our library collection, and added graphics to display intron-splicing efficiency across various tissues, developmental stages, and stress-related conditions. The result is a large collection of 3,313 treatment conditions and 3,594 genetic mutants for discovering differentially regulated splicing efficiency. Our online database can be accessed at https://plantintron.com/.

splicing, RNA-seq, plant, database

Citation: Zhang, H., Jia, J., and Zhai, J. (2023). Plant Intron-Splicing Efficiency Database (PISE): exploring splicing of ~1,650,000 introns in *Arabidopsis*, maize, rice, and soybean from ~57,000 public RNA-seq libraries. Sci China Life Sci 66, 602–611. https://doi.org/10.1007/s11427-022-2193-3

INTRODUCTION

Splicing is an essential process during gene expression in eukaryotes and is performed by a large RNA and protein complex referred to as the spliceosome, which consists of U1, U2, U4, U5, and U6 small nuclear ribonucleoprotein (snRNPs) and other related proteins (Kornblihtt et al., 2013; Laloum et al., 2018). Alternative splicing (AS) is a critical process that expands gene function and plays an important role in plant development and environmental responses (Filichkin et al., 2018; Staiger and Brown, 2013; Syed et al., 2012; Zhang et al., 2017). Intron retention (IR) is the major form of AS in plants (Chamala et al., 2015; Marquez et al., 2012; Mei et al., 2017a; Song et al., 2019), accounting for more than 60% of AS events in *Arabidopsis* (Chaudhary et al., 2019; Reddy et al., 2013), 83% in *Oryza sativa* (Dong et al., 2018), and 56% in maize inbred lines B73 (Mei et al., 2017b). AS also plays an important role in plants in regulating gene expression (Jacob and Smith, 2017), particularly in responding to environmental signals, such as cold, heat, and drought (Chaudhary et al., 2019; Laloum et al., 2018).

In previous studies, researchers have focused on one or a limited number of genetic mutant or environmental stresses

*Corresponding author (email: zhaijx@sustech.edu.cn)

to investigate the effects of AS or IR. These examples include the histone methyltransferase SET DOMAIN GROUP PROTEIN 725 (SDG725) that mediates position-specific IR in rice (Wei et al., 2018), the *OsMet1-2* (methyltransferase 1) mutant that releaved DNA methlylation can affect AS in rice (Wang et al., 2016), and the protein arginine methyltransferases 5 (PRMT5) and Sm-like4 (LSM4) methylation involved in pre-mRNA splicing in *Arabidopsis* (Zhang et al., 2011). Examples of environmental stress include the phytohormone abscisic acid (ABA) signal pathway also plays an important role in response to abiotic stress, the last intron of *HAB1* is retained without ABA and *RBM25* (Cheng et al., 2017; Wang et al., 2015; Zhan et al., 2015). While large-scale raw data has been published in the public database, it is time and energy consuming for most researchers, who may be limited by computer resources or bioinformatics technology, to reanalyze all public RNA-seq data. Although there are some resources for studying AS of plants, such as PastDB, which uses 516 public libraries to analyze gene expression levels and the AS atlas in *Arabidopsis* (Martín et al., 2021), ASIP (Wang and Brendel, 2006) and ERISdb (Szcześniak et al., 2013) which focuses on the characterization of AS events. There is no comprehensive database for investigating intron-splicing efficiency by analyzing all public RNA-seq data of plants, and no resource for users to quickly verify whether genic mutations or treatment conditions affect intron-splicing and whether differences exist between various tissues and developmental stages.

Our previous studies collected over 20,000 *Arabidopsis* RNA-seq public libraries (Zhang et al., 2020) and 45,000 RNA-seq libraries for five other plant species (Yu et al., 2022), which supported an important resource for investigating splicing efficiency. Furthermore, in this study, we established the first ever large-scale splicing efficiency database in four organisms (PISE: https://plantintron.com/), which can reveal the intron-splicing efficiency of selected genes and introns in multiple formats with tables and figures. Additionally, our website includes a web-based Integrative Genomics Viewer (IGV) browser to display the bam files of all ~57,000 libraries stored on our server. Users can select the libraries for display by searching library ID, project ID, or gene ID in our collection.

RESULTS

Building a comprehensive database for plant intron-splicing efficiency

Our database is a collection of over 57,000 public next-generation sequencing (NGS) RNA-seq libraries and the given pipeline for each plant was used to analyze intron-splicing efficiency (IR ratio) (Figure 1A). In addition, we manually curated and annotated all the mutant- and treatment-related libraries and their matched controls included in our library collection, and added graphics to show intron-splicing efficiency across various tissues, developmental stages, and stress-related conditions. Consequently, we obtained a large collection of 3,313 treatment- and 3,594 genetic mutant-related groups to discover the differentially regulated splicing efficiency. Finally, we developed a user-friendly, easily accessible, large-scale database (PISE) to search intron-splicing efficiency (Figure 1B), which includes over 25,000 libraries for *Arabidopsis*, 3,000 for soybean, 17,000 for maize, and 10,000 for rice (Figure 1C).

Overview of splicing information on selected genes

For an overview of all intron-splicing efficiencies of a selected gene, we show the IR ratio among all libraries of selected organisms on the "Information" page, including a box plot of all retained introns of the selected transcript (Figure 2A) and a basic statistical table (Figure 2B). This includes the IR ratio in all libraries for each intron, the median, mean, and the third quartile (Q3) value for each intron. To facilitate access to each intron to scan detailed information, we added a function event for each point in the plot area to show the library name and a function for box clicking to show the IR ratio value of each library. Users can query one intron by clicking the intron ID in the table for more information about the selected intron. Additionally, we changed the function of the legend so that clicking on the legend also displays information on the selected intron. The resulting information on the selected intron is then displayed on the "Data Table" and "Data Plot" pages.

Multi-format of the queried intron

Data Table. After selecting one intron, the "Data Table" page will show detailed information on the IR ratio in all libraries, including sample name, title, IR ratio, reads covered within the intron range, all reads within the intron flank range, ecotype/cultivar, genotype, tissue, project ID, treatment, and release date (Figure 3A). The load table function is supported by canvas-datagrid that provides a right-clicking filtering function for each column. To facilitate filtering, we also added the filter button above the table to support filtering by the reads number of the selected intron, project, tissue, ecotype, and genotype (Figure 3A). Moreover, we supported the table download function to download the details of the selected intron to perform data mining. For example, a previous study reported that the first intron of AT2G17340.1 is largely retained on the *atprmt5* mutant (Deng et al., 2016), and this result is discernible in our database (black point in Figure 3C). In addition, we found that some splicing-related factor mutants or environmental signal-related libraries also have high retention levels on this intron, such as *sac3a-3*

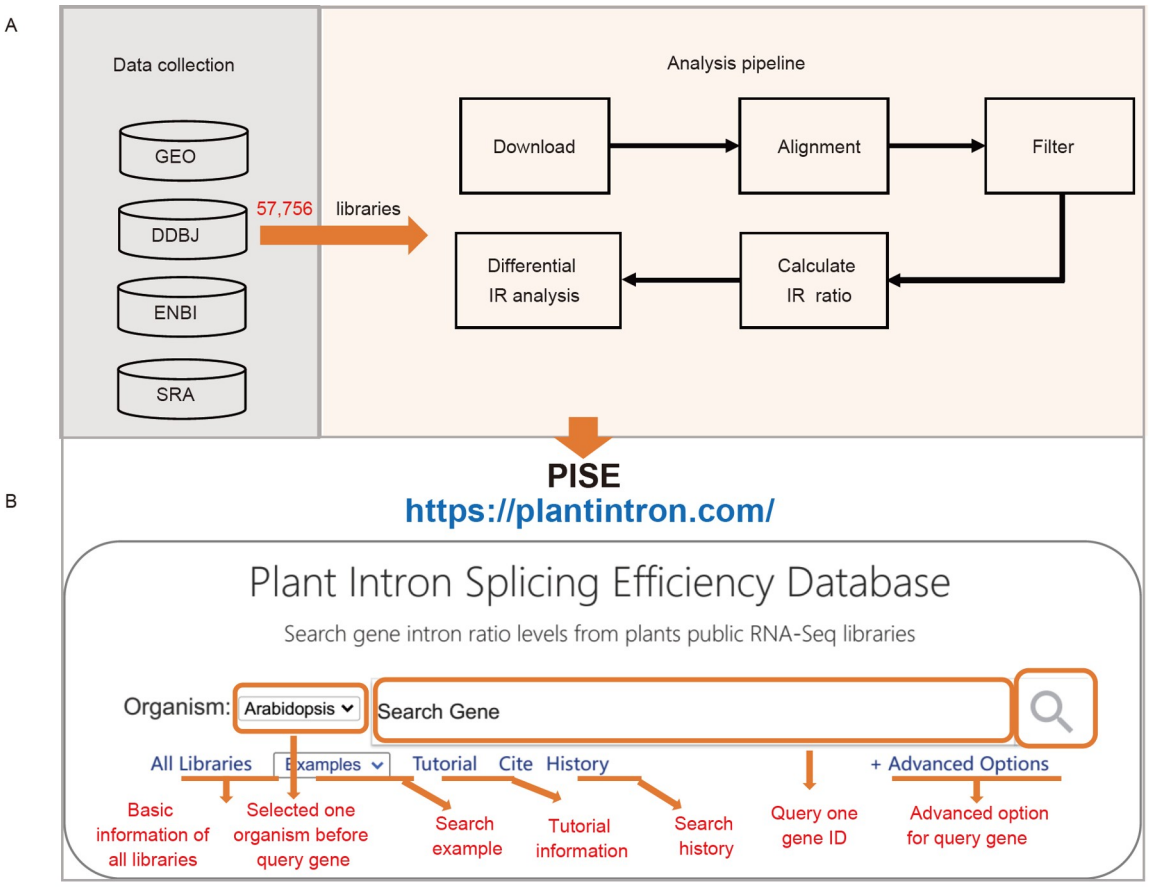

C

Organisms	Total sample	Total Reads (Gb)	Tissue-specific related samples	Treatment-related groups	Mutant-related groups	Intron number
Arabidopsis	25,283	591.38	1,736	1,701	1,860	131,187
Oryza sativa	10,710	300.70	658	903	255	190,232
Zea mays	17,789	406.62	421	611	363	1,064,893
Glycine max	3,974	115.16	498	379	86	266,661
Total	57,756	1,413.86	3,313	3,594	2,564	1,652,973

Figure 1 Overview of Plant Intron-Splicing Efficiency Database (PISE). A, Pipeline of data collection and process. B, Homepage of PISE. C, Statistics on the number of public RNA-seq libraries and introns used in PISE.

(YEAST SAC3 HOMOLOG A) and *prp4a-1(pre-mRNA processing 4 KINASE A)* mutants for heat and cold stress (Figure 3C). There are other mutant libraries, such as *rrc1-3(REDUCED RED-LIGHT RESPONSES IN CRY1CRY2 BACKGROUND 1)*, that may affect the splicing efficiency of this intron and can be determined through experimentation.

Data Plot. To better display the selected intron to the user, "Data Plot" supports multi-format plots to show the intron retention levels, including IR ratio across various tissues, development stages, and biotic and abiotic stresses, as well as the up- or down-regulation between treatment and matched mock, and between mutants and matched wild-type libraries (Figure 3B). In addition, box plots have been used to show the IR ratio between all related samples with regard to tissue-specificity, development stage, and biotic and abiotic stress, and bar plots have been used to display the top 10 groups showing differential intron-splicing efficiency among related mutants and treatments. The figure and corresponding data download function were also supported in the plot area, which allows users to download relevant data by clicking the relevant button (Figure 3B left). Using the first intron of AT2G17340.1 as an example, and by the result of differential intron retention analysis, we found that the intron retention level has been up-regulated under some mutants and treatment conditions, such as *prmt5*, *ant*/*ail6*, *prp4a-1*, and *sac3a-3* mutants, and heat and drought treatments (Figure 3B). This coincides with previously reported retention of this intron in *prmt5* (Deng et al., 2016) and directly

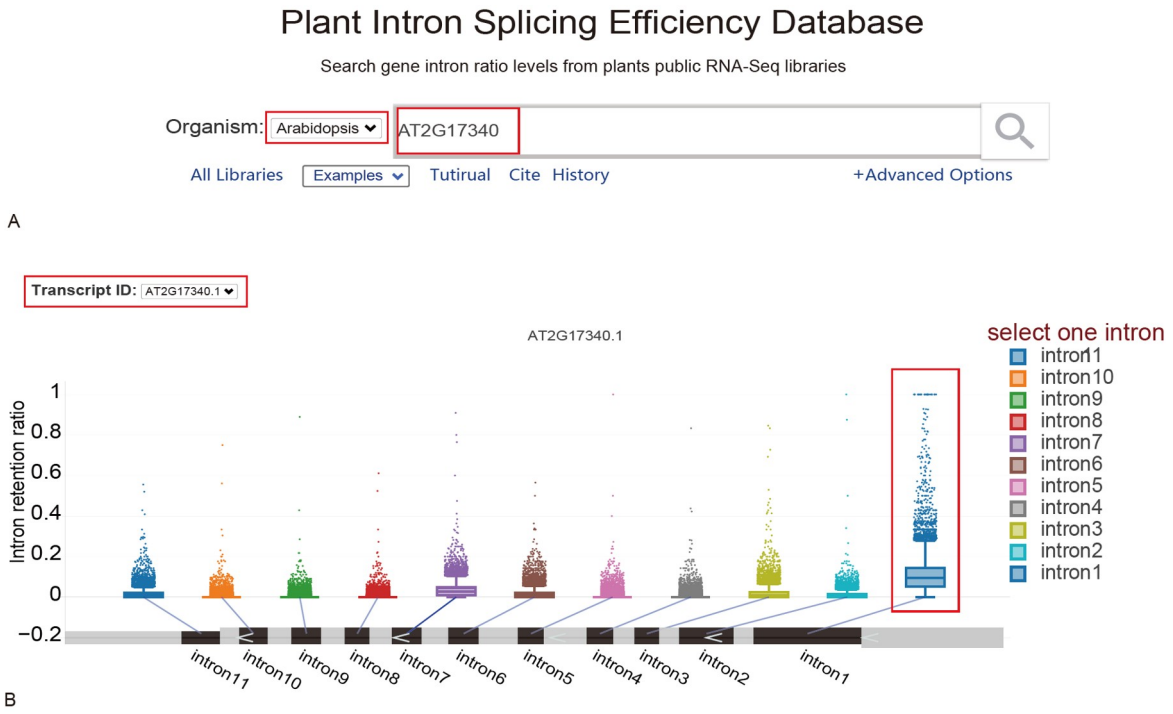

Intron ID	Detected W ith ≥10 Reads	Median	Mean	Q3	Intron Locus
AT2G17340.1_intron11	**19869** of 25283 libraries	0.01	0.0138	0.0200	chr2:7541696-7541820
AT2G17340.1_intron10	**18337** of 25283 libraries	0.00	0.0026	0.0000	chr2:7541884-7541975
AT2G17340.1_intron9	**18789** of 25283 libraries	0.00	0.0030	0.0000	chr2:7542054-7542151
AT2G17340.1_intron8	**19257** of 25283 libraries	0.00	0.0039	0.0000	chr2:7542230-7542308
AT2G17340.1_intron7	**18585** of 25283 libraries	0.03	0.0343	0.0476	chr2:7542384-7542480
AT2G17340.1_intron6	**18354** of 25283 libraries	0.01	0.0157	0.0222	chr2:7542568-7542667
AT2G17340.1_intron5	**18082** of 25283 libraries	0.00	0.0035	0.0000	chr2:7542797-7542879
AT2G17340.1_intron4	**18640** of 25283 libraries	0.00	0.0041	0.0000	chr2:7543021-7543107
AT2G17340.1_intron3	**18150** of 25283 libraries	0.01	0.0182	0.0256	chr2:7543177-7543257
AT2G17340.1_intron2	**17298** of 25283 libraries	0.01	0.0107	0.0151	chr2:7543325-7543500
AT2G17340.1_intron1	**17528** of 25283 libraries	0.09	0.1094	0.1429	chr2:7543567-7543919

Figure 2 Result after querying one gene. A, Box plot of intron retention ratio across AT2G17340.1's intron in *Arabidopsis*. Users can find other transcript intron-splicing levels in all public RNA-seq libraries by changing the "TranscriptID" and can access the plot data by clicking the box. B, Basic information of the drawn intron. The legend in A and "Intron ID" in B both supported the function of searching one intron by clicking intron ID.

overlaps with what was found in the "Data Table".

IGV browser

The "IGV Online" page shows the functionality of the genomics viewer (Robinson et al., 2017). Users can easily view the covered reads for selected genes in all public libraries of the selected organism without any processing of the raw data. For example, we showed the covered reads of *atprmt5* mutant libraries and matched controls of AT2G17340 in *Arabidopsis* (Figure 3D) and found that the coverage of the first intron was considerably higher in the mutant libraries. This result is consistent with the findings shown in Figure 3B and C, thus visually demonstrating the high reliability of our analysis. Furthermore, each button supports an auto-complete function that allows users to search relevant libraries or genes using a keyword or ID.

Comparing splicing efficiency of multiple introns in a single query

PISE supports quick query splicing efficiency of multiple introns at the same time. Here, we used AT2G41760 (*GLN-SPECIFIC AMINO-TERMINAL (NT)-AMIDASE*, *NTAQ1*) as an example, which controls the expression of plant defense-response genes and is involved in the synthetic pathway for the phytoalexin camalexin (Vicente et al., 2019). A previous study found that the IR of the 5th intron of *NTAQ1* significantly increased in the *mac3a*/*3b* double mutant (Tu et al., 2022), which is confirmed in our database (Figure 4A). In addition, we found that the IR of this intron is also up-regulated in *skip*, *lip1*, and *ntr1* mutants (Figure 4A), and the *mac3a*/*3b* mutant libraries also showed higher coverage of the 5th intron (Figure 4C). Interestingly, more reads were covered by the 3rd intron in mutant libraries than in wild-

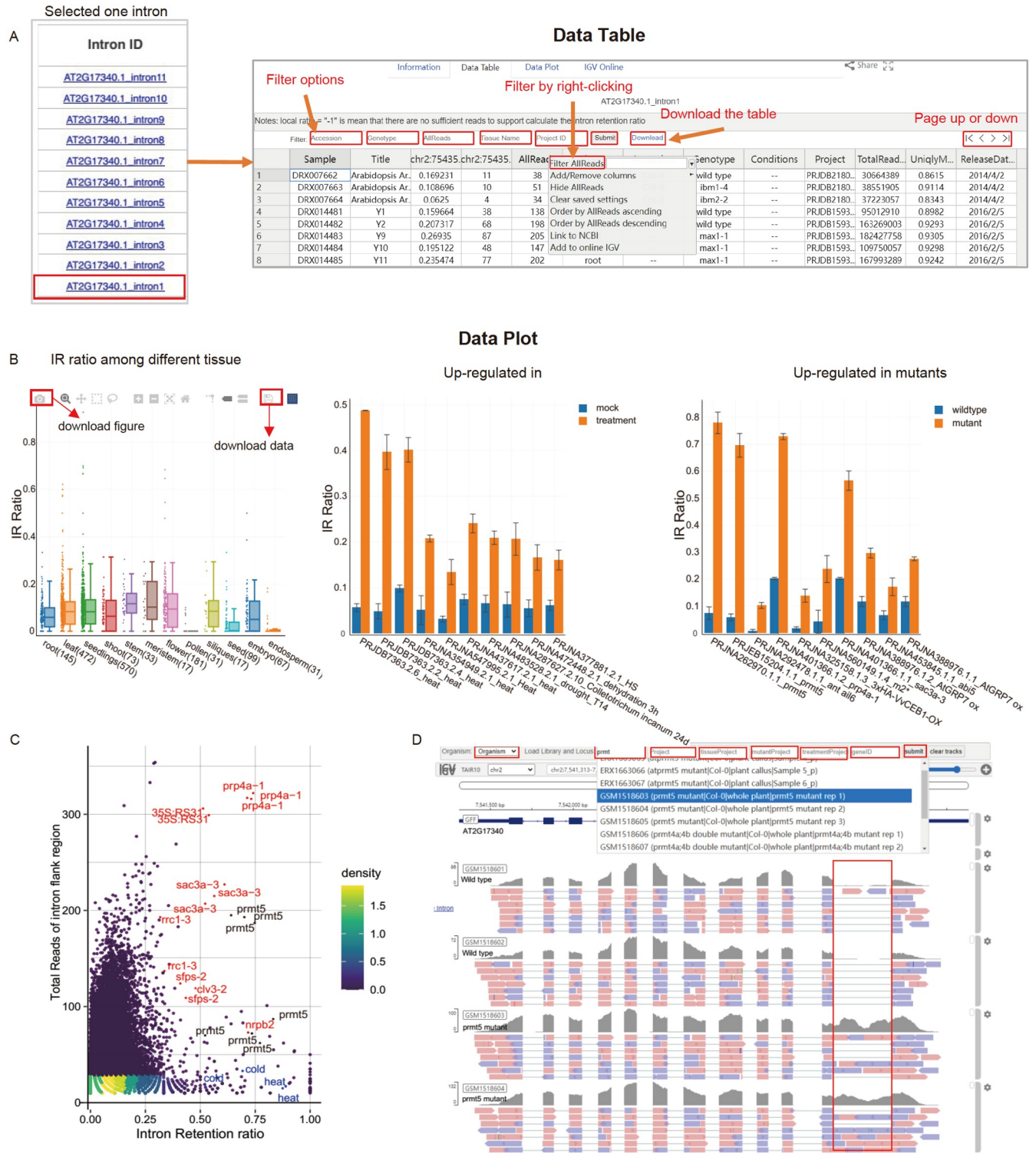

Figure 3 Result of the selected intron. A, Table for the selected intron-splicing efficiency on all public libraries, including library title, project, genotype, ecotype, conditions, the retention ratio, and flanking exon reads. B, Multi-plot of the selected intron (AT2G17340.1#intron1); the left panel is the retention ratio among different tissues, the middle panel is the increased retention level in the top 10 treatment conditions, and the right panel is the up-regulated retention level in the top 10 mutants. C, Intron retention levels of AT2G17340.1#intron1 in all *Arabidopsis* libraries. *prmt5* mutant; the detected IR event of this intron in a previous study was marked black, other mutants with high IR ratios were labeled red, and abiotic stress-related samples with high IR ratio were marked in blue. D, Coverage of AT2G17340 in the selected libraries.

type libraries. Subsequently, the IR ratio levels of the 3rd intron were queried and found that the retention levels also increased in *mac3a*/*3b*, *skip*, and *lip1* mutants, but were not significantly up-regulated in the *ntr1* and *cop1* mutants

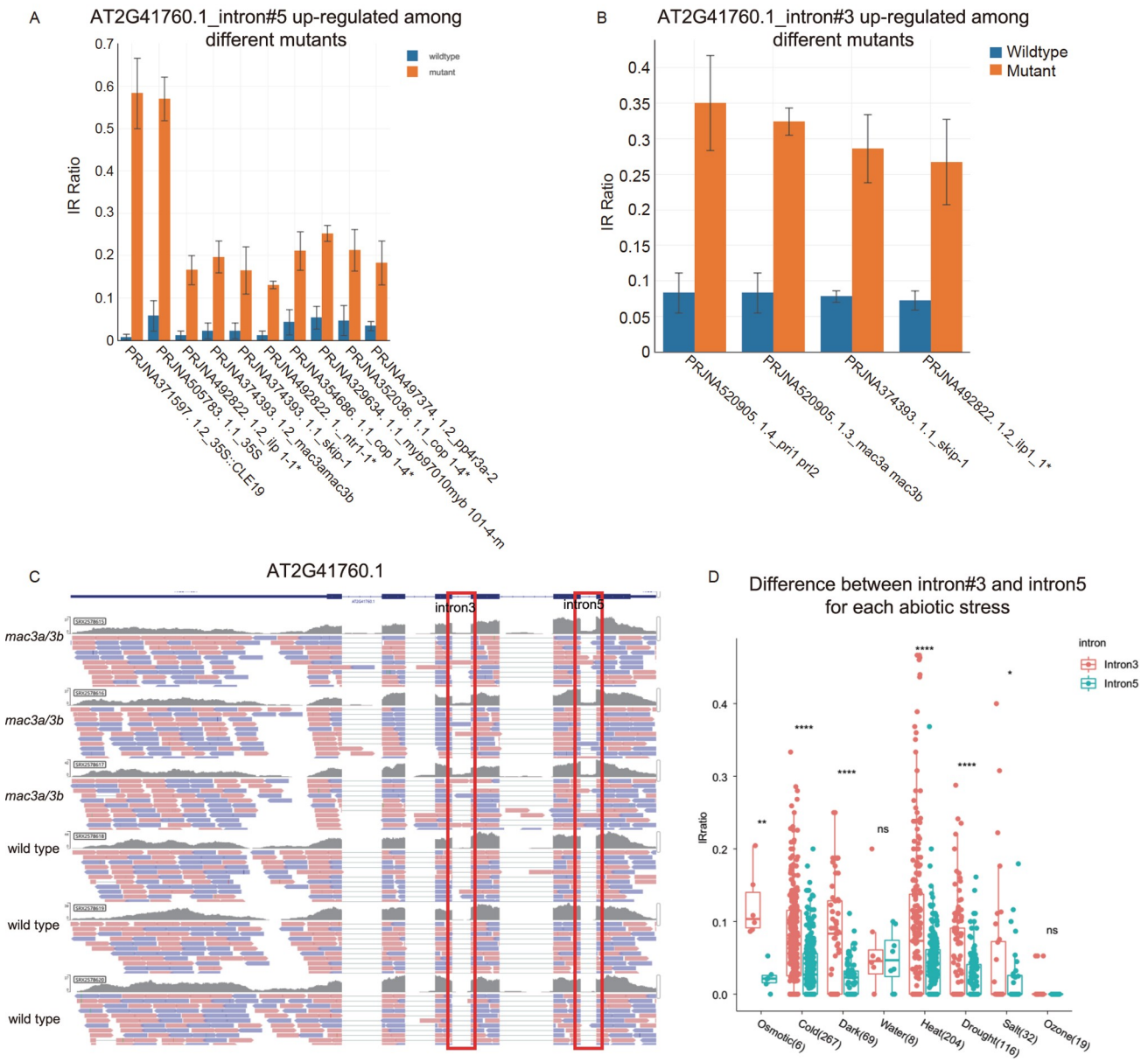

Figure 4 Intron-splicing efficiency of *NTAQ1* (AT2G41760). A and B show the up-regulated IR in different mutants of AT2G41760.1#5 and AT2G41760.1#3, respectively. C, Reads coverage of AT2G41760 in wild-type and *mac3a*/*3b* double mutant libraries. D, Differences in IR of *NTAQ1* 3rd intron and 5th intron at various abiotic stresses, *P*-values calculated by *t*-test (ns: *P*>0.05, *: *P*<=0.05, **: *P*<=0.01, ***: *P*<=0.001, ****: *P*<=0.0001).

(Figure 4B). This difference suggests that the 3rd and 5th introns can be independently regulated by different factors. By comparing the IR ratios between the 3rd and 5th introns under various abiotic stress conditions, we found that the IR ratio levels of introns 3 and 5 are often different (Figure 4D). For example, the IR in the 3rd intron was higher than that in the 5th intron under osmotic stress. These results showed that the retention levels of different introns on the same gene can still differ under the same treatment or stress conditions.

Exploring splicing efficiency in rice, maize, and soybean

In addition to *Arabidopsis*, PISE supports queries for rice, maize, and soybean introns. Users can select the species at the top left of "Homepage" or in "Organism" before querying gene ID. Here, we selected the rice database to query one rice gene, LOC_Os10g11140 (*plastidic phosphor-glucomutase*, *OspPGM*) (Figure 5A), which causes male sterility when it is non-functional (Lee et al., 2016). From an overall view of all intron-splicing efficiency, we found that the IR ratio of different introns among most libraries are lower than 0.2, and outliers of intron#11 were more than those of other introns (Figure 5B left panel). To view the point of intron#11, we clicked the intron#11 box to display the detailed intron retention levels all related libraries (Figure 5B right panel). To query more information about intron#11, we clicked the

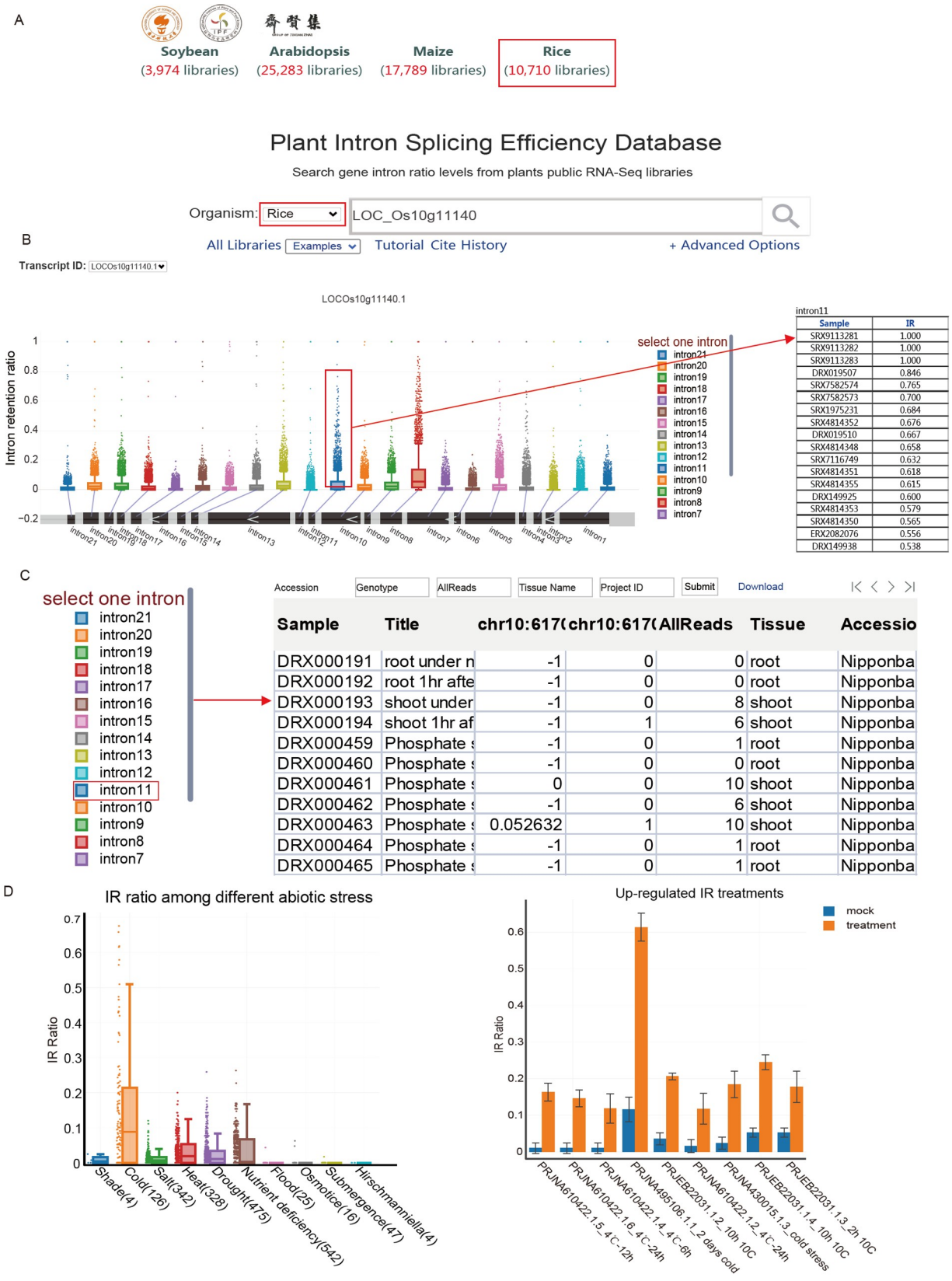

Figure 5 Overview of LOC_Os10g11140 (plastidic phosphoglucomutase, *OsPGM*) intron-splicing efficiency in rice. A, Home page of PISE. B, Left panel shows all intron retention levels among all rice libraries; right panel is a table obtained after clicking box 11 in the plant area. C, Data table of LOC_Os10g11140_intron#11. D, Left panel is the intron-splicing efficiency of LOC_Os10g11140_intron#11 under different abiotic stress; right panel is differential splicing efficiency among different treatment conditions.

button "intron11" in the "select one intron" area, and the "Data Table" and "Data Plot" pages showed the corresponding tables (Figure 5C) and figures (Figure 5D). By analyzing the results of IR ratio under various abiotic stresses, we found that intron-splicing efficiency was reduced under cold stress (Figure 5D left). In addition, the differential splicing efficiency result also indicates that the retention levels of this intron are increased under cold stress (Figure 5D right). These results suggest that cold treatment up-regulates the level of retention of this intron, which may affect its fertility under cold stress.

DISCUSSION

In the present study, we support a free comprehensive database for rapidly scanning plant intron-splicing efficiency. Users can easily access splicing information for a particular intron in public data without any data processing, including the number of reads supporting intron retention, the treatments that will up- or down-regulate the splicing efficiency, and whether the intron is specifically regulated during tissue and developmental stages. Although some resources for investigating plant AS are available, they either focus on the splicing site features (Szcześniak et al., 2013; Wang and Brendel, 2006) or only use 516 public libraries to study the splicing atlas (Martín et al., 2021). Our database uses larger-scale public data and shows the intron-splicing efficiency using data tables and figures of four plants in multiple formats, making it more user-friendly to obtain valid information that is of interest.

This way, most researchers with a limited background in bioinformatics can benefit from our website, which uses a "data-driven, hypothesis-generating" approach without the need for performing sophisticated informatics analysis, and devise testable experimental hypotheses based on novel information extracted from such a comprehensive database. For example, the first intron of AT2G17340.1 was reported to be retained in the *Arabidopsis prmt5* mutant (Deng et al., 2016), and our database confirmed this result using *prmt5* mutant libraries and discovered many other potential regulators for this intron from the mutant analysis (Figure 3B and C). Therefore, PISE provides a concise, user-friendly, "Google-style" search function to query gene intron-splicing efficiency, allowing users to easily obtain information on their gene of interest or intron splicing levels under various specifications of tissues, development stages, stresses, treatments, and genetic mutants.

MATERIAL AND METHODS

Data collection and process

We collected the public RNA-seq data from the Gene Expression Omnibus (GEO), Sequence Read Archive (SRA), European Nucleotide Archive (ENA), and DNA Data Bank of Japan databases (DDBJ) for *Arabidopsis*, rice, maize, and soybean till 2020, and then manually went through all libraries to complete the basic information and filter some libraries which may include small RNAs (smRNAs) or long non-coding RNAs (lncRNAs). The raw data were aligned to the reference genome using HISAT2 (Kim et al., 2015), and the TAIR10, Williams 82, B73 v4, and MSU 7 genomes were used as references for *Arabidopsis*, soybean, maize, and rice, respectively. Subsequently, libraries with low mapped reads (unique mapped reads <1M) were discarded. Finally, we used over 57,000 libraries (Figure 1C) to perform downstream analysis. Only genes with at least one intron were used for analysis, and the intron-splicing efficiency (IR ratio) was calculated using a python script from Jia (Jia et al., 2020). All intron information was extracted from published annotation files, including Araport11 for *Arabidopsis*, B73 v4 for maize, MSU 7 for rice, and Williams 82 a2 for soybean.

Differential intron-splicing efficiency analysis

After filtering, we manually curated and annotated all the mutant- and treatment-related libraries as well as their matched controls included in our library collection and added graphics to display intron-splicing efficiency across different tissues, developmental stages, and stress-related conditions for *Arabidopsis*, maize, rice, and soybean. The result was a large collection of 3,313 treatment conditions and 3,594 genetic mutants for discovering the differentially regulated splicing efficiency (Figure 1C), with at least two libraries with more than 1M mapped reads for the control and treatment/mutant groups. The generalized linear model in DESeq2 (Love et al., 2014) was used to calculate the fold-change and *P*-value for each intron and for use in the IRFinder test (Middleton et al., 2017), and the Benjamini Hochberg method was used to adjust the *P*-value (*P*-adj). The fold change and *P*-adj were filtered for each intron before being plotted on the "Data Plot" page.

PISE website and database

MySQL and LMDB were used as storage units to hold all relevant data tables for querying genes or libraries, including the basic information of the library, gene information, and corresponding values of intron-splicing efficiency. Php, HTML, and JavaScript were used to build a web framework that connected the PC and server. To better display the data, we upgraded the function of Plotly.js to plot all figures and support downloading and displaying the corresponding data, and added a filter button in canvas-datagrid.js to upload the data table. We used the parameters "*P*-adj<0.05 and mean of

control or experiment group IR ratio ≥0.1" to filter all related groups for mutant- and treatment-related plots and plot the libraries of the retained groups. To conveniently view the coverage of one gene of selected online libraries, the online genomic browser was supported using igv.js (Robinson et al., 2017), which supports library ID, project ID, treatments, mutants, tissue group IDs, and keywords to search the library of interest.

Compliance and ethics *The author(s) declare that they have no conflict of interest.*

Acknowledgements *We thank all the research groups that contributed RNA-seq data to the community, and we regret not being able to cite all the related papers in the main text owing to space constraints. References for all libraries used are listed in PISE 'All Libraries'. Computation was supported by Center for Computational Science and Engineering at Southern University of Science and Technology. The group of J.Z. was supported by the National Key R&D Program of China (2019YFA0903903), the Program for Guangdong Introducing Innovative and Entrepreneurial Teams (2016ZT06S172), the Shenzhen Sci-Tech Fund (KYTDPT20181011104005), the Key Laboratory of Molecular Design for Plant Cell Factory of Guangdong Higher Education Institutes (2019KSYS006), and the Stable Support Plan Program of Shenzhen Natural Science Fund (20200925153345004). J.J. was supported by the National Natural Science Foundation of China (32100444) and the Shenzhen Fundamental Research Program (JCYJ20210324105202007).*

References

Chamala, S., Feng, G., Chavarro, C., and Barbazuk, W.B. (2015). Genome-wide identification of evolutionarily conserved alternative splicing events in flowering plants. Front Bioeng Biotechnol 3, 33.

Chaudhary, S., Khokhar, W., Jabre, I., Reddy, A.S.N., Byrne, L.J., Wilson, C.M., and Syed, N.H. (2019). Alternative splicing and protein diversity: plants versus animals. Front Plant Sci 10, 708.

Cheng, C., Wang, Z., Yuan, B., and Li, X. (2017). RBM25 mediates abiotic responses in plants. Front Plant Sci 8.

Deng, X., Lu, T., Wang, L., Gu, L., Sun, J., Kong, X., Liu, C., and Cao, X. (2016). Recruitment of the NineTeen complex to the activated spliceosome requires AtPRMT5. Proc Natl Acad Sci USA 113, 5447–5452.

Dong, C., He, F., Berkowitz, O., Liu, J., Cao, P., Tang, M., Shi, H., Wang, W., Li, Q., Shen, Z., et al. (2018). Alternative splicing plays a critical role in maintaining mineral nutrient homeostasis in rice (*Oryza sativa*). Plant Cell 30, 2267–2285.

Filichkin, S.A., Hamilton, M., Dharmawardhana, P.D., Singh, S.K., Sullivan, C., Ben-Hur, A., Reddy, A.S.N., and Jaiswal, P. (2018). Abiotic stresses modulate landscape of poplar transcriptome via alternative splicing, differential intron retention, and isoform ratio switching. Front Plant Sci 9, 5.

Jacob, A.G., and Smith, C.W.J. (2017). Intron retention as a component of regulated gene expression programs. Hum Genet 136, 1043–1057.

Jia, J., Long, Y., Zhang, H., Li, Z., Liu, Z., Zhao, Y., Lu, D., Jin, X., Deng, X., Xia, R., et al. (2020). Post-transcriptional splicing of nascent RNA contributes to widespread intron retention in plants. Nat Plants 6, 780–788.

Kim, D., Langmead, B., and Salzberg, S.L. (2015). HISAT: a fast spliced aligner with low memory requirements. Nat Methods 12, 357–360.

Kornblihtt, A.R., Schor, I.E., Alló, M., Dujardin, G., Petrillo, E., and Muñoz, M.J. (2013). Alternative splicing: a pivotal step between eukaryotic transcription and translation. Nat Rev Mol Cell Biol 14, 153–165.

Laloum, T., Martín, G., and Duque, P. (2018). Alternative splicing control of abiotic stress responses. Trends Plant Sci 23, 140–150.

Lee, S.K., Eom, J.S., Hwang, S.K., Shin, D., An, G., Okita, T.W., and Jeon, J.S. (2016). Plastidic phosphoglucomutase and ADP-glucose pyrophosphorylase mutants impair starch synthesis in rice pollen grains and cause male sterility. J Exp Bot 67, 5557–5569.

Love, M.I., Huber, W., and Anders, S. (2014). Moderated estimation of fold change and dispersion for RNA-seq data with DESeq2. Genome Biol 15, 550.

Marquez, Y., Brown, J.W.S., Simpson, C., Barta, A., and Kalyna, M. (2012). Transcriptome survey reveals increased complexity of the alternative splicing landscape in *Arabidopsis*. Genome Res 22, 1184–1195.

Martín, G., Márquez, Y., Mantica, F., Duque, P., and Irimia, M. (2021). Alternative splicing landscapes in *Arabidopsis thaliana* across tissues and stress conditions highlight major functional differences with animals. Genome Biol 22, 35.

Mei, W., Boatwright, L., Feng, G., Schnable, J.C., and Barbazuk, W.B. (2017a). Evolutionarily conserved alternative splicing across monocots. Genetics 207, 465–480.

Mei, W., Liu, S., Schnable, J.C., Yeh, C.T., Springer, N.M., Schnable, P.S., and Barbazuk, W.B. (2017b). A comprehensive analysis of alternative splicing in paleopolyploid maize. Front Plant Sci 8, 694.

Middleton, R., Gao, D., Thomas, A., Singh, B., Au, A., Wong, J.J.L., Bomane, A., Cosson, B., Eyras, E., Rasko, J.E.J., et al. (2017). IRFinder: assessing the impact of intron retention on mammalian gene expression. Genome Biol 18, 51.

Reddy, A.S.N., Marquez, Y., Kalyna, M., and Barta, A. (2013). Complexity of the alternative splicing landscape in plants. Plant Cell 25, 3657–3683.

Robinson, J.T., Thorvaldsdóttir, H., Wenger, A.M., Zehir, A., and Mesirov, J.P. (2017). Variant review with the integrative genomics viewer. Cancer Res 77, e31–e34.

Song, Q.A., Catlin, N.S., Brad Barbazuk, W., and Li, S. (2019). Computational analysis of alternative splicing in plant genomes. Gene 685, 186–195.

Staiger, D., and Brown, J.W.S. (2013). Alternative splicing at the intersection of biological timing, development, and stress responses. Plant Cell 25, 3640–3656.

Syed, N.H., Kalyna, M., Marquez, Y., Barta, A., and Brown, J.W.S. (2012). Alternative splicing in plants—coming of age. Trends Plant Sci 17, 616–623.

Szcześniak, M.W., Kabza, M., Pokrzywa, R., Gudyś, A., and Makałowska, I. (2013). Erisdb: a database of plant splice sites and splicing signals. Plant Cell Physiol 54, e10.

Tu, Y.T., Chen, C.Y., Huang, Y.S., Chang, C.H., Yen, M.R., Hsieh, J.W.A., Chen, P.Y., and Wu, K. (2022). HISTONE DEACETYLASE 15 and MOS4-associated complex subunits 3A/3B coregulate intron retention of ABA-responsive genes. Plant Physiol 190, 882–897.

Vicente, J., Mendiondo, G.M., Pauwels, J., Pastor, V., Izquierdo, Y., Naumann, C., Movahedi, M., Rooney, D., Gibbs, D.J., Smart, K., et al. (2019). Distinct branches of the N-end rule pathway modulate the plant immune response. New Phytol 221, 988–1000.

Wang, B.B., and Brendel, V. (2006). Genomewide comparative analysis of alternative splicing in plants. Proc Natl Acad Sci USA 103, 7175–7180.

Wang, X., Hu, L., Wang, X., Li, N., Xu, C., Gong, L., and Liu, B. (2016). DNA methylation affects gene alternative splicing in plants: an example from rice. Mol Plant 9, 305–307.

Wang, Z., Ji, H., Yuan, B., Wang, S., Su, C., Yao, B., Zhao, H., and Li, X. (2015). ABA signalling is fine-tuned by antagonistic HAB1 variants. Nat Commun 6, 8138.

Wei, G., Liu, K., Shen, T., Shi, J., Liu, B., Han, M., Peng, M., Fu, H., Song, Y., Zhu, J., et al. (2018). Position-specific intron retention is mediated by the histone methyltransferase SDG725. BMC Biol 16, 44.

Yu, Y., Zhang, H., Long, Y., Shu, Y., and Zhai, J. (2022). Plant Public RNA-seq Database: a comprehensive online database for expression analysis

of ~45000 plant public RNA-Seq libraries. Plant Biotechnol J 20, 806–808.

Zhan, X., Qian, B., Cao, F., Wu, W., Yang, L., Guan, Q., Gu, X., Wang, P., Okusolubo, T.A., Dunn, S.L., et al. (2015). An *Arabidopsis* PWI and RRM motif-containing protein is critical for pre-mRNA splicing and aba responses. Nat Commun 6, 8139.

Zhang, H., Zhang, F., Yu, Y., Feng, L., Jia, J., Liu, B., Li, B., Guo, H., and Zhai, J. (2020). A comprehensive online database for exploring ~20,000 public *Arabidopsis* RNA-Seq libraries. Mol Plant 13, 1231–1233.

Zhang, R., Calixto, C.P.G., Marquez, Y., Venhuizen, P., Tzioutziou, N.A., Guo, W., Spensley, M., Entizne, J.C., Lewandowska, D., Ten Have, S., et al. (2017). A high quality *Arabidopsis* transcriptome for accurate transcript-level analysis of alternative splicing. Nucl Acids Res 45, 5061–5073.

Zhang, Z., Zhang, S., Zhang, Y., Wang, X., Li, D., Li, Q., Yue, M., Li, Q., Zhang, Y., Xu, Y., et al. (2011). *Arabidopsis* floral initiator SKB1 confers high salt tolerance by regulating transcription and pre-mRNA splicing through altering histone H4R3 and small nuclear ribonucleoprotein LSM4 methylation. Plant Cell 23, 396–411.